Available online at www.sciencedirect.com
ScienceDirect
Trans. Nonferrous Met. Soc. China 29(2019) 1424−1429
Transactions of Nonferrous Metals Society of China
www.tnmsc.cn

Effect of deep surface rolling on microstructure and properties of AZ91 magnesium alloy

Xian LUO[1], Qi-yang TAN[2], Ning MO[2], Yu YIN[2], Yan-qing YANG[1], Wyman ZHUANG[3], Ming-xing ZHANG[2]

1. School of Materials Science and Engineering, Northwestern Polytechnical University, Xi'an 710072, China;
2. School of Mechanical and Mining Engineering, The University of Queensland, St. Lucia, QLD 4072, Australia;
3. Aerospace Division, Defence Science and Technology,
506 Lorimer Street, Fishermans Bend, Victoria 3207, Australia

Received 13 November 2018; accepted 25 April 2019

Abstract: A solution-treated AZ91 bulk material was deep-surface-rolled at room temperature to investigate the effect of deep surface rolling on the microstructure and mechanical properties of the alloy. Microhardness and microstructure along the depth of the treated surface layer were characterized. The results show that the affected layer was up to 2.0 mm thick and consisted of three sublayers: a severe deformation layer with thickness of about 400 μm from the topmost surface, a medium deformation layer with thickness of around 600 μm and a small deformation layer up to 1000 μm thick. In addition to grain refinement in the deformation layer, strain-induced precipitation of β phase ($Mg_{17}Al_{12}$) was observed, particularly in the severe and medium deformation layers. It is believed that the cooperative effects of grain refinement, strain hardening and precipitation strengthening led to the significant increase in hardness of the AZ91 alloy after the deep surface rolling.

Key words: surface deformation; magnesium alloy; deep surface rolling; microstructural evolution; hardness

1 Introduction

Because surface strengthening can significantly improve hardness, wear and fatigue resistance of metallic materials, surface nanocrystallization has been considered as an emerging approach to achieve superior surface properties [1−3] in addition to conventional techniques for metal surface strengthening, such as shot peening and rolling. In the past years, various surface nanocrystallization techniques have been well developed, including surface mechanical grinding treatment (SMGT) or surface mechanical attrition treatment (SMAT) [2−4], ultrasonic shot peening [5], high energy shot peening (HESP) [6], supersonic rolling [7] and laser shock processing [8], etc.

AZ91 Mg alloy (Mg−9wt.%Al−1wt.%Zn) is the most widely used cast magnesium alloy due to its superior combination of castability, mechanical properties and low cost [9]. There have been some studies on surface nanocrystallization of AZ91 alloy by SMAT or HESP [10−12]. The grain refinement mechanisms have been well established. However, the severe deformation layer (surface nanocrystallization layer) produced by SMAT or HESP is usually very thin (less than 100 μm), and the surface is generally associated with high surface roughness and micro-cracks. Especially, little attention has been paid to the precipitation behavior of β phase ($Mg_{17}Al_{12}$) during the surface nanocrystallization process.

Deep surface rolling (DSR), also known as deep rolling (DR), is a well-developed and widely-used mechanical surface treatment method to produce compressive residual stress on the surface of metallic component in order to improve fatigue life [13−15]. The major advantage of DSR over other surface treatment techniques is its thick affected layer (about 1−3 mm). Hence, it is a very suitable method for surface nanocrystallization treatment. In addition, after DSR, the treated surface has low surface roughness (≤1 μm) and

Foundation item: Project (2016ZE53046) supported by the Aviation Science Foundation of China; Project (201606295009) supported by the China Scholarship Council; Project supported by Top International University Visiting Program for Outstanding Young Scholars of Northwestern Polytechnical University, China
Corresponding author: Xian LUO, Tel: +86-13519134551, E-mail: luoxian@nwpu.edu.cn;
Ming-xing ZHANG, Tel: +61-733468709, E-mail: mingxing.zhang@uq.edu.au
DOI: 10.1016/S1003-6326(19)65049-1

almost no microcracks [16,17]. ALTENBERGER et al [18] studied the effect of deep rolling on the cyclic performance of magnesium alloys in the temperature range from 20 to 250 °C. Their results showed that deep rolling led to pronounced enhancement of fatigue life at room temperature. However, the microstructure was not well characterized. The present work aims to investigate and understand the effects of DSR on the microstructure and mechanical property evolutions in the surface layer of an AZ91 Mg alloy.

2 Experimental

In order to avoid the influence of secondary phase, a commercial AZ91 Mg alloy ingot was solid-solution-treated at 420 °C for 48 h and followed by water quenching to form single phase alloy. Then, the ingot was cut and machined into 100 mm × 60 mm × 10 mm plates for the DSR processing. The DSR device is a hydraulic rolling device. Figure 1(a) shows the DSR process on a CNC milling machine. Figure 1(b) illustrates how a hydraulically-floated ball was used to press on the top surface of an AZ91 sample. The detailed DSR processing parameters are: the roller is a spherical high strength steel ball with a diameter of 13 mm; the rolling pressure is 10 MPa, and the rolling feed rate is 1400 mm/min. The rolling paths used in this study were twice in the longitudinal direction (LD) and then twice in the transverse direction (TD), and the distance between neighbouring paths is 0.056 mm, with a schematic diagram shown in Fig. 2(a). The LD plus TD processing can make the surface layer of the sample have uniform deformation and isotropic microstructure in the process plane. During the DSR process, the sample was cooled by coolant. The DSR parameters are derived from the research work [19]. After the DSR, the surface of the sample is smooth and has a mirror surface finish, as shown in Fig. 2(b). R_a≤0.27 μm was achieved according to our test by a TA620 roughness measuring platform. So, DSR can obtain high surface finish.

The average grain size of top surface layer of the deep-rolled sample was analyzed in terms of peak width on the X-ray diffraction (XRD) spectra [20]. The XRD was conducted on a Bruker Advance D8 X-ray diffractometer with Cu K_α radiation within the 2θ range from 30° to 80° with a step of 0.02°. Variation of hardness along the depth from the treated surface was measured using a Struers Duramin Vickers hardness testing machine, with a load of 25 g and a loading time of 10 s. At each depth, at least three tests were carried out and the average hardness was presented with a standard deviation.

The cross-sectional microstructures of the sample were examined using a POLYVAR MET optical microscope (OM) and JEOL JSM−7001F field-emission scanning electron microscope (SEM). For OM and SEM analyses, the samples were cut, mounted, polished successively and then etched by 2 vol.% nital. The

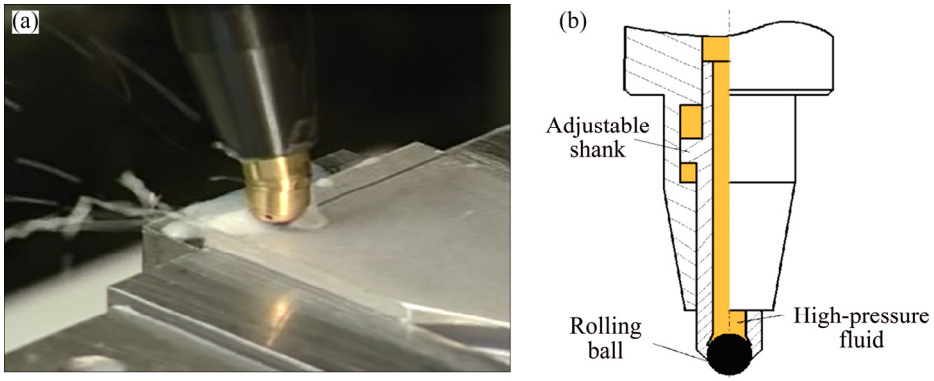

Fig. 1 DSR process on top surface of sample using CNC milling machine (a) and schematic illustration of DSR tool (b)

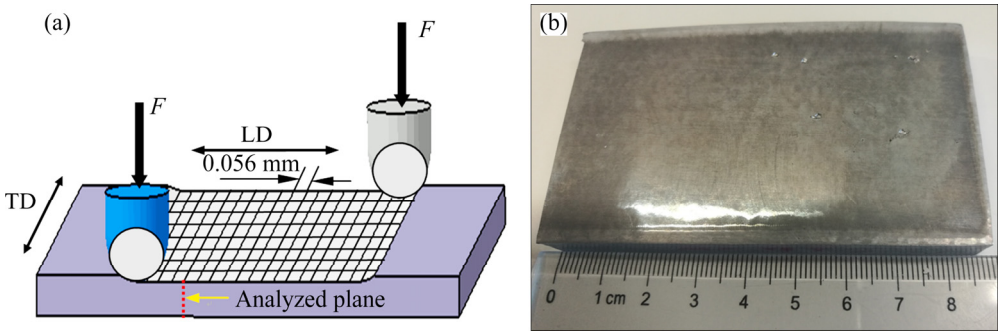

Fig. 2 Schematic diagram showing processing directions and analyzed plane (a) and image showing processed surface of AZ91 Mg alloy (b)

detailed microstructure in the severe deformation layer was also analyzed with JEM−2100 transmission electron microscope (TEM). A FEI Dual FIB/SEM-SCIOS focused ion beam (FIB) equipment was used to prepare the TEM foil at a depth of about 20 μm from the topmost surface of the DSRed sample. It should be pointed out that both hardness and microstructure analyses are on the plane shown in Fig. 2(a).

3 Results and discussion

3.1 Macrostructure analyses

The XRD patterns of the solution-treated AZ91 magnesium alloy before and after the DSR are shown in Fig. 3. The XRD spectra only show single HCP α-Mg solid solution. However, after the DSR, distinct broadenings of the Bragg reflections appear, implying a grain refinement, microstrain development and micro-distortions of the crystalline lattice [11]. The average grain size, in terms of Scherrer equation $D=K\lambda/(L_s\cos\theta)$ (where D is grain size, L_s is full-width-half-max (FWHM) of the diffraction peak, θ is the diffraction angle, K is constant (0.9), and λ is wavelength of the X-ray) [20], is 28.3 nm. This result agrees with previously-published result from SMAT technique [10].

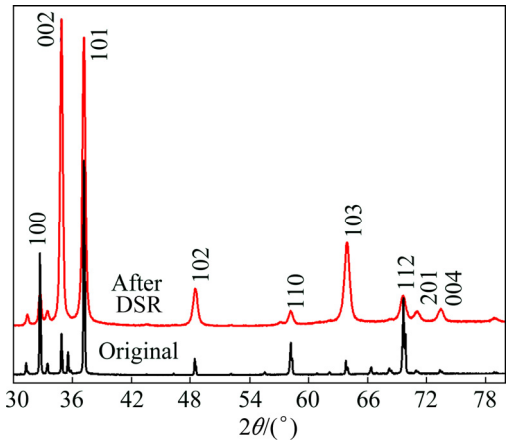

Fig. 3 XRD patterns of solution-treated AZ91 magnesium alloy before and after DSR

A typical cross-sectional OM micrograph of the DSRed sample is shown in Fig. 4(a). It can be seen that the entire affected layer is up to 2 mm thick, which can be divided into three sublayers. The first sublayer is the severe deformation layer from the topmost surface, which is about 400 μm thick. It looks relatively dark and completely different from the substrate under OM after the chemical etching. This sublayer corresponds to the nanocrystalline or sub-micrometer scaled grains. The next sublayer is the medium deformation layer, which is about 600 μm thick. In this region, the staggered deformation twins can be clearly seen, and the density of twins is gradually decreased along the depth. The small deformation layer is close to the substrate, which is up to 1000 μm thick and is associated with low density of deformation twins.

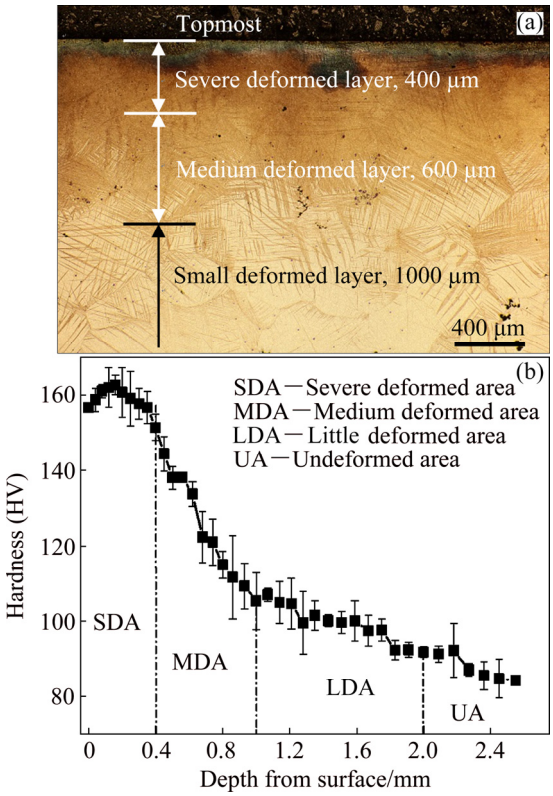

Fig. 4 Cross-sectional optical micrograph close to deep-rolled surface (a) and hardness profile from topmost surface to substrate (b)

The variation of micro-hardness with distance from the topmost surface to the substrate is plotted in Fig. 4(b). It can be seen that the hardness distribution corresponds well to the microstructure of Fig. 4(a). The severe deformation layer has the highest hardness, which is twice that of the substrate. The degree of enhancement is the same as that of the SMAT [10]. However, the severe deformation layer with high hardness is much thicker than the nanocrystalline layer produced by conventional SMAT. The latter is just around 100 μm [10]. In addition, it is interesting to see that the micro-hardness distribution in the severe deformation layer firstly increases and then decreases mildly, and the highest hardness appears at the subsurface (in the depth of around 0.2 mm). MEYER et al [21,22] also found the similar phenomena after the material X210Cr12 (AISI D3) was treated by DSR. They explained that the phenomena resulted from the characteristics of Hertzian stress and the big ball diameter applied in the DR process. The gradient hardness variation in the medium deformation layer and small deformation layer is distinctly related to the gradually-decreased deformation extent.

3.2 Microstructure analyses

In order to further investigate the microstructure in the deformation layer, SEM and TEM studies were conducted. Figure 5 shows cross-sectional SEM images of the deformation layer at different depths. Continuous precipitates (white particles) along the deformation twin boundaries can be clearly observed. The amount and size of the precipitates decrease along the depth (see Figs. 5(a−d)). The large and high density precipitates basically distribute homogeneously in the severe deformation layer (see Fig. 5(a)) due to the high density of crystal defects (mainly twins and dislocations). These fine and high density of precipitates should contribute to the hardness improvement of the DSRed sample.

In order to identify the precipitates and verify the refined grains in the severe deformation layer, TEM examination was conducted at the depth of about 20 μm from the topmost surface. Figure 6(a) shows a typical bright-field TEM micrograph and Fig. 6(b) indicates the corresponding selected-area electron diffraction (SAED) pattern. The approximate diffraction rings indicate that randomly-oriented grains are obtained. Both α-Mg and $Mg_{17}Al_{12}$ phases are identified by carefully indexing the SAED pattern. The rings 2−3 and 5−7 are the overlapped diffractions of α-Mg and $Mg_{17}Al_{12}$. The ring 2 corresponds to $(0002)_{Mg}$ and $(400)_{\beta}$. The ring 3 corresponds to $(10\bar{1}1)_{Mg}$ and $(411)_{\beta}$, which are generally the strongest diffractions of the two phases. The ring 5 corresponds to $(10\bar{1}2)_{Mg}$ and $(521)_{\beta}$, the ring 6 corresponds to $(11\bar{2}0)_{Mg}$ and $(541)_{\beta}$, and the ring 7 corresponds to $(10\bar{1}3)_{Mg}$ and $(721)_{\beta}$. The diffraction spots at ring 4 correspond to $(332)_{\beta}$ only. The other diffraction spots on rings 1 and 8 are from α-Mg, as shown in Fig. 6(b). Therefore, the nanometer or submicron scale grains shown in Fig. 6(a) consist of α-Mg grains and β particles. The result indicates that, within the severe deformation layer during deep rolling processing, not only the nanocrystallization or grain refinement occurs, but also the precipitation of $Mg_{17}Al_{12}$ phase is induced. However, there are still some high-strain-energy subgrains that have not been transformed into nanograins, as indicated in regions A and B in Fig. 6(a). Therefore, the significant enhancement of the hardness in the severe deformation layer is resulted from the grain refinement, precipitation strengthening and strain strengthening. Similar to the SMAT of AZ91 alloy [10], the grain refinement process can be divided into three steps: twinning, which divides the coarse grains into twin platelet; then formation of subgrains and dislocation arrays as subgrain boundaries through dislocation movements, and dynamic recrystallization to form nano-sized grains at last. The grains such as the “clean” nanometer grain (marked C) around a high strain area (marked B) in Fig. 6(a) show the evidence of dynamic recrystallization process.

In order to further confirm the strain-induced precipitation of the β phase, a scanning transmission electron microscopy (STEM) image of the severe

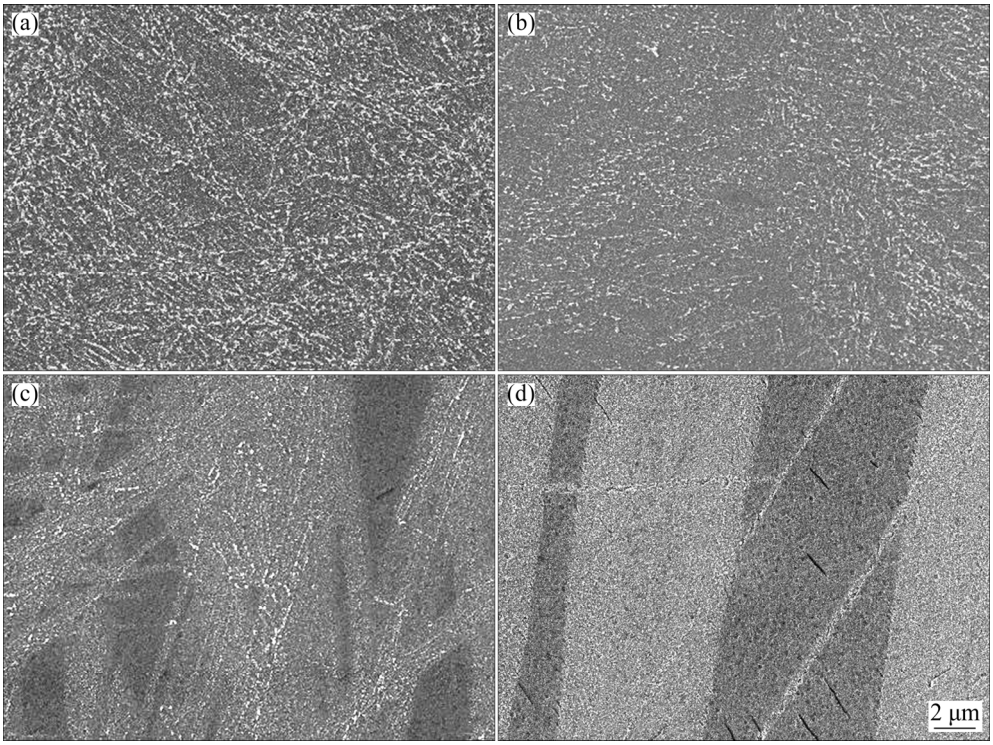

Fig. 5 Cross-sectional SEM images of deep-surface-rolled sample showing precipitates at different depths: (a) Close to topmost surface; (b) ~0.5mm; (c) ~1.0 mm; (d) ~1.5 mm

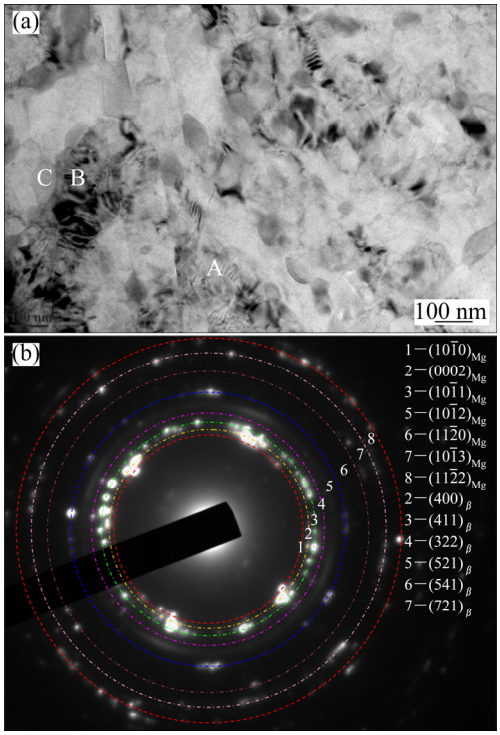

Fig. 6 Bright-field TEM image showing refined nanograins or precipitated $Mg_{17}Al_{12}$ particles with some severely deformed subgrains (a) and corresponding SAED pattern showing coexistence of polycrystalline α-Mg and β phase (b)

deformed layer and corresponding energy-dispersive X-ray spectroscopy (EDS) mapping of elements were obtained, as shown in Fig. 7. In Fig. 7(a), the bright particles distribute along certain directions (should be twin boundaries) different from the matrix. EDS mapping of Al element shown in Fig. 7(b) indicates that these bright particles are enriched with Al. Thus, these particles are determined to be $Mg_{17}Al_{12}$ precipitates.

The strain-induced β-$Mg_{17}Al_{12}$ precipitation was scarcely reported during cold deformation or conventional SMAT processes in solution treated AZ91 magnesium alloy [10,23]. The presently used deep rolling processing was associated with high pressure and relatively slow rolling speed. This possibly produced more heat energy due to friction and improved the temperature of the affected layer [24]. Moreover, the deformation led to high density of crystal defects, such as dislocations, lattice vacancy and twins, which promoted the diffusion of solute atoms. Thus, it is considered that the elevated temperature and high density of crystal defects during deep rolling process were responsible for the strain-induced precipitation. From a thermodynamic point of view, the formation energy of $Mg_{17}Al_{12}$ is negative in the entire temperature range (0−700 K) [25]. So, β phase can be also produced at lower temperatures in thermodynamics view.

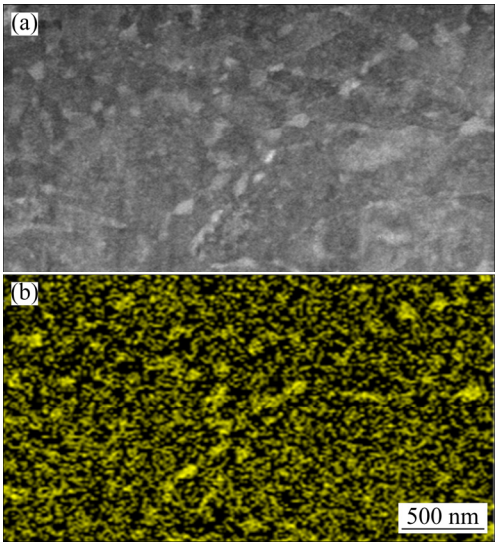

Fig. 7 STEM micrograph (a) and Al mapping result indicating distributions of β phase (b)

In order to exclude that the precipitation phenomenon is just a kind of natural ageing, we repeated the experiments from DSR processing to microstructural observations in 10 d, and our results approved the reproducibility of the precipitation phenomenon of β phase.

4 Conclusions

(1) The solution-treated AZ91 magnesium alloy had a 2.0 mm-thick affected layer after the deep surface rolling. The affected layer can be divided into three sublayers: the severe deformation layer of about 400 μm deep from the topmost surface, the medium deformation layer of about 600 μm thick in the middle of the deformation layer, and the small deformation layer of about 1000 μm thick next to the undeformed base material.

(2) In the deformation layer, the severe deformation sublayer in particular, in addition to the grain refinement and increase in density of crystal defects, strain-induced precipitation of $Mg_{17}Al_{12}$ phase also occurred. Thus, the high hardness of the severe deformation layer is attributed to the cooperative effects of grain refinement, work hardening and precipitation hardening.

References

[1] FANG T H, LI W L, TAO N R, LU K. Revealing extraordinary intrinsic tensile plasticity in gradient nano-grained copper [J]. Science, 2011, 331: 1587−1590.

[2] LIU X C, ZHANG H W, LU K. Strain-induced ultrahard and ultrastable nanolaminated structure in nickel [J]. Science, 2013, 342: 337−340.

[3] ZHANG Le-hao, ZOU Yun, WANG Hong-tao, MENG Liang, LIU Jian-bin, ZHANG Zhong-wu. Surface nanocrystallization of

Mg−3wt.%Li−6wt.%Al alloy by surface mechanical attrition treatment [J]. Materials Characterization, 2016, 120: 124−128.
[4] LI W L, TAO N R, LU K. Fabrication of a gradient nano−micro-structured surface layer on bulk copper by means of a surface mechanical grinding treatment [J]. Scripta Materialia, 2008, 59: 546−549.
[5] WU X, TAO N, HONG Y, XU B, LU J, LU K. Microstructure and evolution of mechanically-induced ultrafine grain in surface layer of Al-alloy subjected to USSP [J]. Acta Materialia, 2002, 50: 2075−2084.
[6] LIU G, WANG S C, LOU X F, LU J, LU K. Low carbon steel with nanostructured surface layer induced by high-energy shot peening [J]. Scripta Materialia, 2001, 44: 1791−1795.
[7] CHENG Ming-long, ZHANG De-yuan, CHEN Hua-wei, QIN Wei, LI Jin-sheng. Surface nanocrystallization and its effect on fatigue performance of high-strength materials treated by ultrasonic rolling process [J]. The International Journal of Advanced Manufacturing Technology, 2016, 83: 123−131.
[8] LOU S, LI Y, ZHOU L, NIE X, HE G, LI Y, HE W. Surface nanocrystallization of metallic alloys with different stacking fault energy induced by laser shock processing [J]. Materials & Design, 2016, 104: 320−326.
[9] KIRAN G V, KRISHNA K H, SAMEER S, BHARGAVI M, KUMAR B S, RAO G M, NAIDUBABU Y, DUMPALA R, SUNIL B R. Machining characteristics of fine grained AZ91 Mg alloy processed by friction stir processing [J]. Transactions of Nonferrous Metals Society of China, 2017, 27: 804−811.
[10] SUN H Q, SHI Y N, ZHANG M X, LU K. Plastic strain-induced grain refinement in the nanometer scale in a Mg alloy [J]. Acta Materialia, 2007, 55: 975−982.
[11] HOU Li-feng, WEI Ying-hui, LIU Bao-sheng, XU Bing-she. Microstructure evolution of AZ91D induced by high energy shot peening [J]. Transactions of Nonferrous Metals Society of China, 2008, 18: 1053−1057.
[12] LALEH M, KARGAR F. Effect of surface nanocrystallization on the microstructural and corrosion characteristics of AZ91D magnesium alloy [J]. Journal of Alloys and Compounds, 2011, 509: 9150−9156.
[13] ALTENBERGER I. Deep rolling−The past, the present and the future [C]// Proceedings of the 9th International Conference on Shot Peening. Paris, France, 2005: 144−155.
[14] ZHUANG W Z, HALFORD G R. Investigation of residual stress relaxation under cyclic loading [J]. International Journal of Fatigue, 2001, 23(S): s31−s37.
[15] ZHUANG W, LIU Q, DJUGUM R, SHARP P K, PARADOWSKA A. Deep surface rolling for fatigue life enhancement of laser clad aircraft aluminium alloy [J]. Applied Surface Science, 2014, 320: 558−562.
[16] NIKITIN I, ALTENBERGER I, MAIER H J, SCHOLTES B. Mechanical and thermal stability of mechanically induced near-surface nanostructures [J]. Materials Science and Engineering A, 2005, 403: 318−327.
[17] JUIJERM P, ALTENBERGER I. Fatigue performance enhancement of steels using mechanical surface treatments [J]. Journal of Metals, Materials and Minerals, 2007, 17: 59−65.
[18] ALTENBERGER I, WAGNER L, MHAEDE M, JUIJERM P, NOSTER U. Effect of deep rolling on the cyclic performance of magnesium and aluminum alloys in the temperature range 20−250 ºC [C]// 10th International Conference on Shot Peening. Tokyo, Japan, 2008: 557−562.
[19] ZHUANG W, WICKS B. Multipass low-plasticity burnishing induced residual stresses: Three-dimensional elastic-plastic finite element modeling [J]. Proceedings of the Institution of Mechanical Engineers: Part C, 2004, 218(6): 663−668.
[20] LUO Jun, ZHU Hang-tian, LIANG Jing-kui. Determination of crystallite size and strain by X-ray powder [J]. Physics, 2009, 38(4): 267−275. (in Chinese)
[21] MEYER D, BRINKSMEIER E, HOFFMANN F. Surface hardening by cryogenic deep rolling [J]. Procedia Engineering, 2011, 19: 258−263.
[22] MEYER D. Cryogenic deep rolling – An energy based approach for enhanced cold surface hardening [J]. CIRP Annals−Manufacturing Technology, 2012, 61: 543−546.
[23] HOU Li-feng, WEI Ying-hui, LIU Bao-sheng, XU Bing-she. High energy impact techniques application for surface grain refinement in AZ91D magnesium alloy [J]. Journal of Materials Science, 2008, 43: 4658−4665.
[24] SALAHSHOOR M, GUO Y B. Process Mechanics in Deep Rolling of Magnesium-Calcium (MgCa) Biomaterial [C]//ASME 2011 International Manufacturing Science and Engineering Conference. Corvallis, USA, 2011: 303−311.
[25] ZHUANG H, CHEN M, CARTER E A. Elastic and thermodynamic properties of complex Mg−Al intermetallic compounds via orbital-free density functional theory [J]. Physical Review Applied, 2016, 5: 064021.

表面深滚处理对 AZ91 镁合金组织及性能的影响

罗 贤[1]，Qi-yang TAN[2]，Ning MO[2]，Yu YIN[2]，杨延清[1]，Wyman ZHUANG[3]，Ming-xing ZHANG[2]

1. 西北工业大学 材料学院，西安 710072；
2. School of Mechanical and Mining Engineering, The University of Queensland, St. Lucia, QLD 4072, Australia；
3. Aerospace Division, Defence Science and Technology, 506 Lorimer Street, Fishermans Bend, Victoria 3207, Australia

摘 要：在室温下对固溶处理后的 AZ91 镁合金块体材料进行表面深滚处理，以研究其对合金表面显微组织和力学性能的影响。分析被加工试样表层沿深度方向的显微硬度和显微组织。结果表明，表面影响层厚度达到 2.0 mm，可分为 3 个亚层：从最表面起约为 400 μm 厚的严重变形层，大约 600 μm 厚的中等变形层和厚度达 1000 μm 的小变形层。在变形层中除晶粒细化外，还观察到应变诱导析出的 β 相($Mg_{17}Al_{12}$)，尤其是在严重变形层和中等变形层内。研究认为，晶粒细化、应变硬化和沉淀强化的协同作用使 AZ91 镁合金在表面深滚后的硬度显著提高。

关键词：表面变形；镁合金；表面深滚；显微组织演变；硬度

(Edited by Bing YANG)